



Next Generation Very Large Array Memo No. 112
April 2023

High Dynamic Range Imaging at 8 GHz at 1mas Resolution

C.L. Carilli

National Radio Astronomy Observatory, Socorro, NM, USA

Abstract

I investigate the ability of the ngVLA to make high dynamic range images at VLBI resolution of a complex, extended source with high and low surface brightness regions. The model is a doctored version of the best Cygnus A image at 8 GHz from the VLA, scaled to be $\sim 0.75''$ in maximum extent, implying a spatial dynamic range for the simulated observation (source size/spatial resolution) of ~ 750 . The configuration includes all antennas in LONG and MID, plus 10 Spiral antennas and 5 core antennas. The results are encouraging: the image dynamic range (peak/rms) is 1.5×10^4 , and the fidelity across most of the source is better than 5%. The ngVLA has good Fourier plane coverage over a remarkable range of spatial frequencies. The resulting VLBI-resolution ngVLA image is comparable in quality to high-quality images produced with current many element, connected interferometers, such as the Jansky Very Large Array.

1 Introduction

One of the unique aspects of the ngVLA is the continuity of Fourier spacing coverage from ~ 100 m to 10^9 m, implying sensitivity to structures over a range of 10^7 in angular scale, just for the 18 m array itself. I do not believe there is any combination of existing arrays (eg. the HSA or the EVN) that

provide such complete and continuous UV coverage over such a large spatial range.

In this study I investigate the ability of the ngVLA to image a complex source with structures over a large range in spatial frequency, including regions of high and low surface brightness.

2 Model and Simulation

The source model is an adapted version of the VLA high dynamic range image of Cygnus A at 8 GHz. The image has a total flux density of 241 Jy, at an intrinsic resolution of $0.3''$.

Total true source extent is $120''$, which implies intrinsic spatial dynamic range of the input image of $120/0.3 = 400$. However, the radio core is intrinsically very compact. Hence, I blank the core region and replace it with a point source at the core flux density of 1 Jy. The pixel size is then scaled to obtain an image total extent of $\sim 0.75''$. This scales the input model resolution down to ~ 1.8 mas, which is comparable to the resolution of the simulated observations; meaning most of the structures of the input model, except the radio core, have been 'pre-convolved' with a beam comparable in size to the synthesized beam. The model image is shown in Figure 1.

Given the minimum to maximum baseline range of the ngVLA, one could push the spatial DNR in the input model even further. However, that would require an input model with a higher intrinsic spatial dynamic range. Further, the processing already involves large images (8k). Making the model even just a factor 3 larger in angle would make the processing prohibitive.

The intrinsic dynamic range of the input image is $\sim 10^4$. However, the image is then blanked at the 4σ level, with further by-hand blanking of higher residuals around the dominant hot spots at the end of the lobes, resulting in a model with no extraneous structures other than the radio source. While the blanking process can be considered subjective, the fact remains that, whether using a doctored real-source model image, or a fabricated source of random geometric structures, the goal is simply to reproduce as closely as possible this input model, as judged by the resulting imaging artifacts and fidelity.

From a single frequency image, I generate a model spectral cube of 2 GHz total bandwidth with 10 spectral channels, centered at 8 GHz. For simplicity, a flat spectrum was assumed (complex spectral structure should be investigated further). For a real observation, 200 MHz channels would lead to significant bandwidth smearing (relative to the resolution) at the radius

of the Cygnus A hot spots in the model. However, SIMOBSERVE knows nothing of bandwidth smearing nor time smearing — each time record and frequency channel are set at the center of the channel and time record. Hence, the averaging time and channel width were adopted to reduce processing time but enable a multifrequency and time synthesis.

CASA SIMOBSERVE was used to generate the visibility measurement sets. A 5 hour synthesis was employed with a record length of 60 seconds. The synthesis was centered at transit at OV (roughly the center of LONG in longitude), and the source declination was set to $+50^\circ$, to ensure mutual visibility for all antennas throughout.

For the configuration, I employ all the antennas in the LONG (30 antennas in 10 stations, maximum baseline ~ 9000 km), and MID (46 antennas, maximum baseline ~ 1000 km), configurations as currently defined in Revision E. I then include 10 antennas from Spiral, including all 5 antennas at the ends of the arms (maximum baseline ~ 40 km), and another 5 spiraling in to the Core. I include 5 antennas from the Core, with baselines down to a few hundred meters. LONG itself includes intra-station baselines that extend down to ~ 50 m. The number of Spiral and Core antennas was adopted to follow roughly the flux density ratio on the short baselines to that on the long baselines, although the choice was certainly not optimized. I call this the LONG++ configuration, for ease of reference.

Thermal noise is not added to the simulation, in order to focus the analysis on dynamic range limitations due to the image restoration process, particularly gridding and deconvolution, ie. Fourier spacing coverage and interpolation. The measured off-source rms noise in the resulting image due to these effects is still well above that expected for thermal noise.

2.1 Results

Images were generated with TCLEAN using a multifrequency synthesis, with Briggs weighting and a robust parameter of -1, using a CLEAN box around the source and 200000 iterations. The resulting image is shown in Figure 2, and the PSF in Figure 3.

The Gaussian fit to the PSF in CASA has a $\text{FWHM} = 2.05 \text{ mas} \times 0.91 \text{ mas}$ at -9.2° . For comparison, a NA weighted beam has $\text{FWHM} = 4.7 \text{ mas} \times 3.3 \text{ mas}$ at 58° , while $R = 0$ has $2.4 \text{ mas} \times 1.1 \text{ mas}$ at -9° . Both NA and $R = 0$ resulted in a total flux density for the source (integrated over a box encompassing the whole source), at least a factor two larger than in the input model. This extra flux is due to a positive bias, or plateau, across the full image due to the very short spacings being given significant weight.

The PSF in both cases shows very broad positive skirts (see Figure 3 and Rosero ngVLA memos 55 and 65). A multi-scale CLEAN, and making a larger image, might mitigate this effect.¹

The image in Figure 2 has a peak surface brightness of 1.1 Jy beam^{-1} , and an off-source rms noise of $71 \mu\text{Jy beam}^{-1}$, implying an image dynamic range of 1.5×10^4 . The total flux density is 249 Jy, within 3% of the model. Figure 2 also shows an expanded view of the radio jet, demonstrating the high quality of the resulting image, reproducing complex, faint structure with a quality comparable to a full synthesis with multiple configurations of the VLA. The peak residuals around the point source radio core are $< 0.5\%$.

The image fidelity, defined as: $(\text{Model} - \text{Image})/\text{Model}$, where the Model has been convolved with the Gaussian CLEAN beam, is shown in Figure 4. The image fidelity is high across the source, with an rms of about 2% over the higher surface brightness regions, and 6% in the fainter tails of the radio lobes. The rms fidelity even across the faint, narrow jet is 13%.

As a final test, I made an image using just the LONG inter-station baselines (without the internal station baselines)². The resulting image of the Northern hot spot region is shown in Figure 5. Only the hot spot region is shown because the LONG inter-station baselines do not sample any other structures in the source: the shortest projected inter-station baseline in LONG is about 300 km (HI-KU), implying that LONG-alone only samples structures smaller than ~ 20 mas, which is about the size of the hot spots in the scaled model.

Figure 6 shows the uv-coverage for the LONG++ configuration, and also the coverage for the LONG inter-station baselines. LONG in isolation has a central hole with radius $\sim 300\text{km}$, corresponding to a spatial frequency of ~ 20 mas, and generally sparse coverage below 1000 km baselines, corresponding to about 6 mas scales. The LONG++ configuration has complete uv-coverage down to Core-scales (100's of meters). On the other hand, for imaging of sources with structures smaller than 10 mas to 20 mas, the LONG-only uv-coverage including bandwidth synthesis (25% bandwidth), is good.

The conclusion is that, if one wants to image sources with structures larger than 20mas or so at 8GHz with the ngVLA, one needs the Mid and

¹A multi-scale CLEAN was attempted, but deemed impossible slow.

²Including the internal station baselines, which are ~ 100 m, corresponding to a spatial resolution typically $\sim 1'$, is comparable to including just a total power measurement, then jumping to baselines of 300 km or longer. Again, this total power measurement simply introduces a positive bias across the entire field, but adds no information on scales relevant to the model source structures.

even shorter baselines. Note that uv-weighting doesn't help if the information on given spatial scales just doesn't exist. Fortunately, the ngVLA is designed with excellent uv-coverage from ~ 100 m to 9000 km, and the image quality, even at VLBI-type resolution, will be comparable to the best connected element interferometers today.

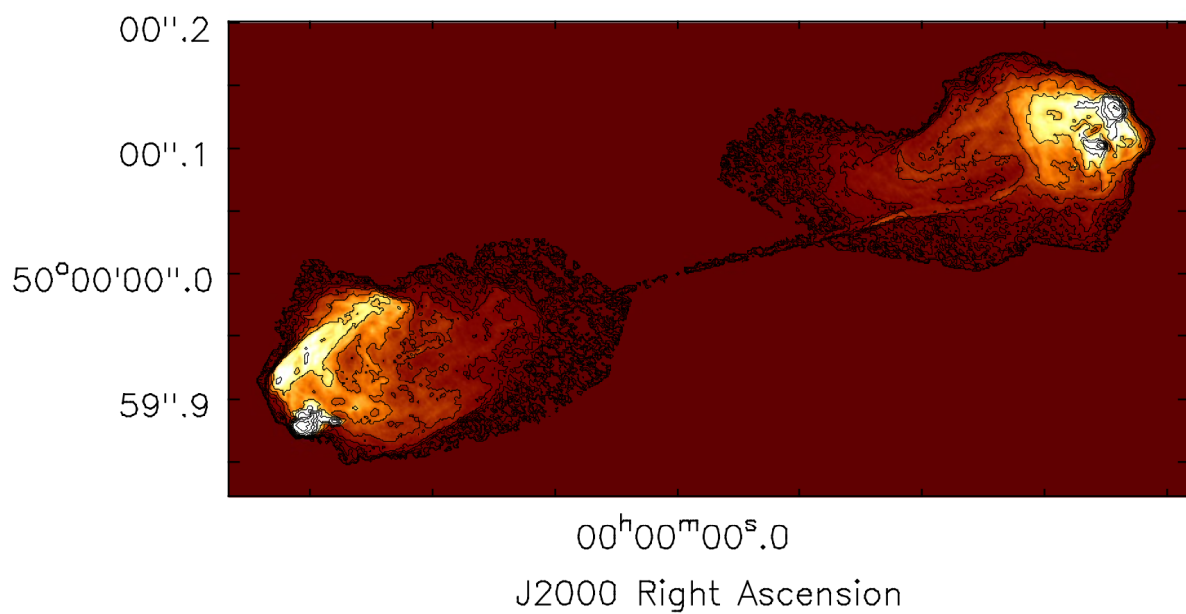


Figure 1: Input model for the ngVLA 8GHz simulations. The contour levels are a geometric progression in factor two starting at $4 \mu\text{Jy pixel}^{-1}$. The scaled intrinsic resolution of the model has FWHM ~ 1.8 mas.

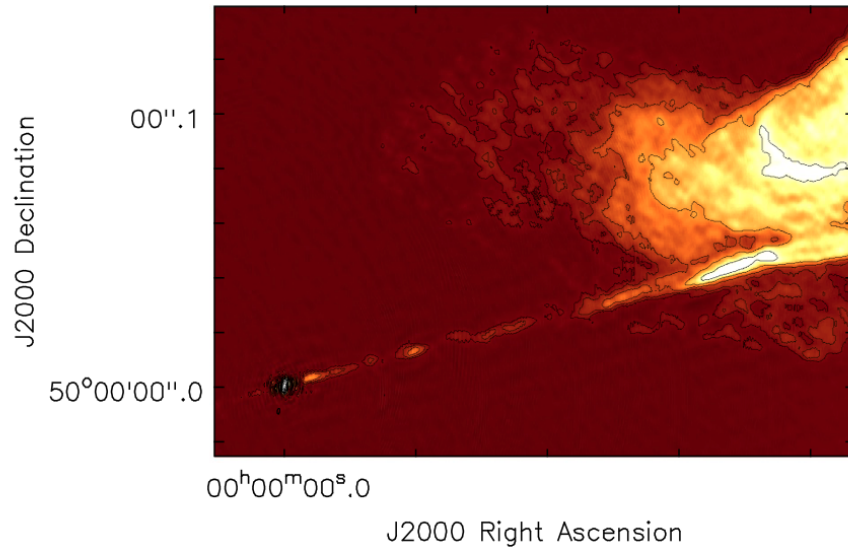
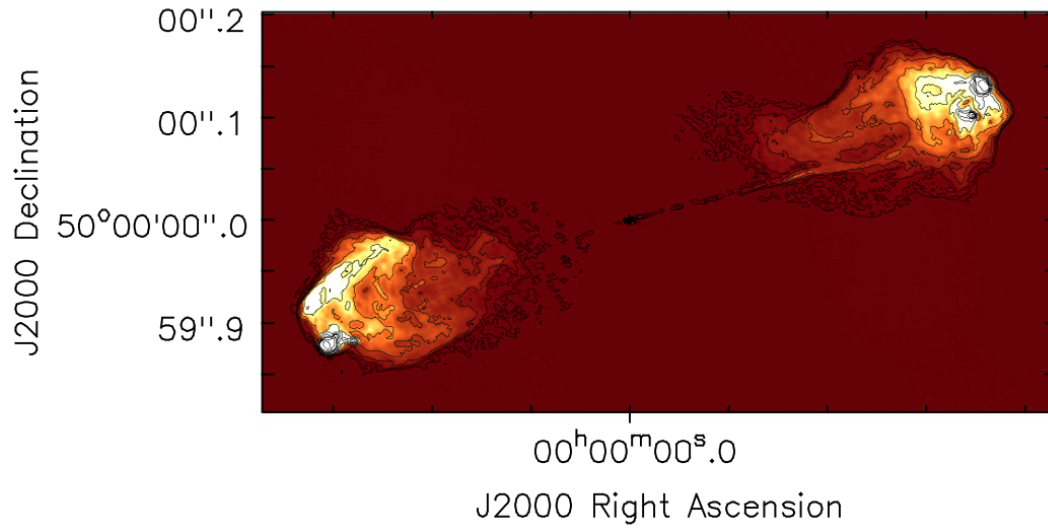


Figure 2: Top: ngVLA 8GHz image using LONG++ of the scaled Cygnus A model. Bottom: expanded view of the jet. The contour levels are a geometric progression in factor two starting at $0.3 \text{ mJy beam}^{-1}$. Negative contours are dashed. The PSF Gaussian fit is: $2.05 \text{ mas} \times 0.91 \text{ mas}$ at -9.2° .

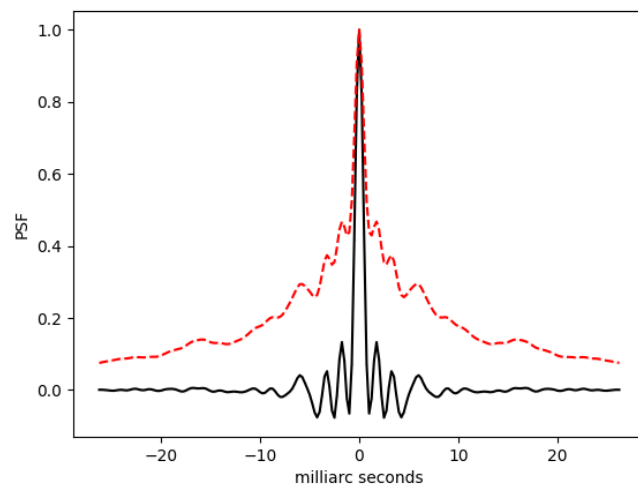


Figure 3: East-West cut through the synthesized beam of LONG++. Black is for $R=-1$ and red (dash) is $R=2$.

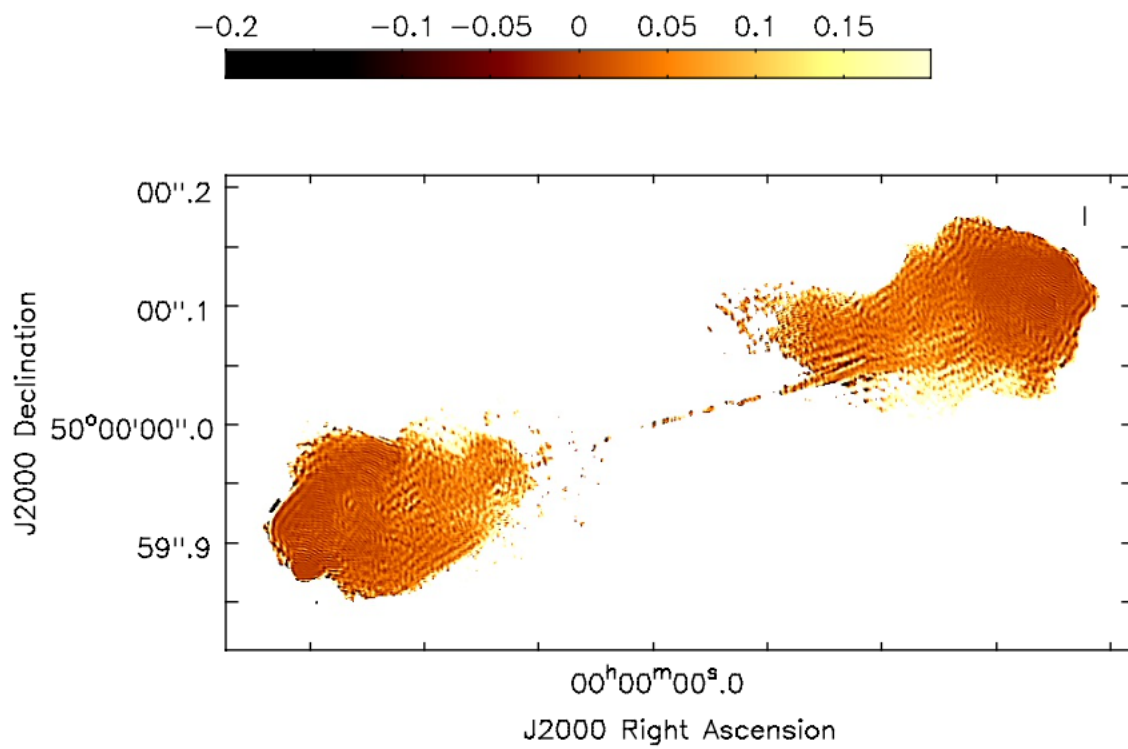


Figure 4: Fidelity image, as defined in section 2.

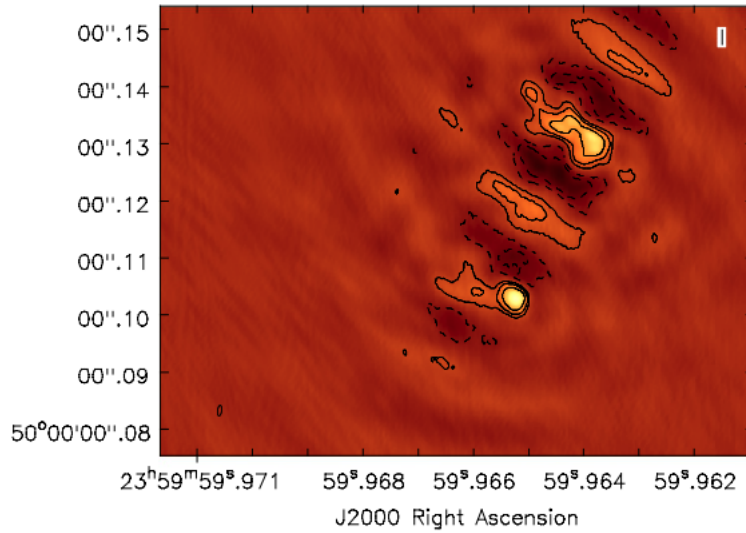
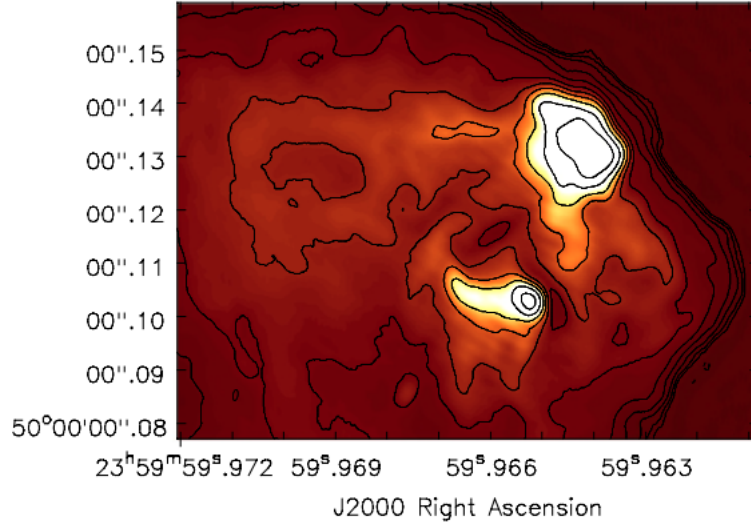


Figure 5: Top: ngVLA 8GHz image of the northern hot spots regions of the Cygnus A model. The contour levels are a geometric progression in factor two starting at $0.3 \text{ mJy beam}^{-1}$. Bottom: same, but using just LONG baselines, without MID or any other antennas. The starting contour level is now 30 mJy beam^{-1} .

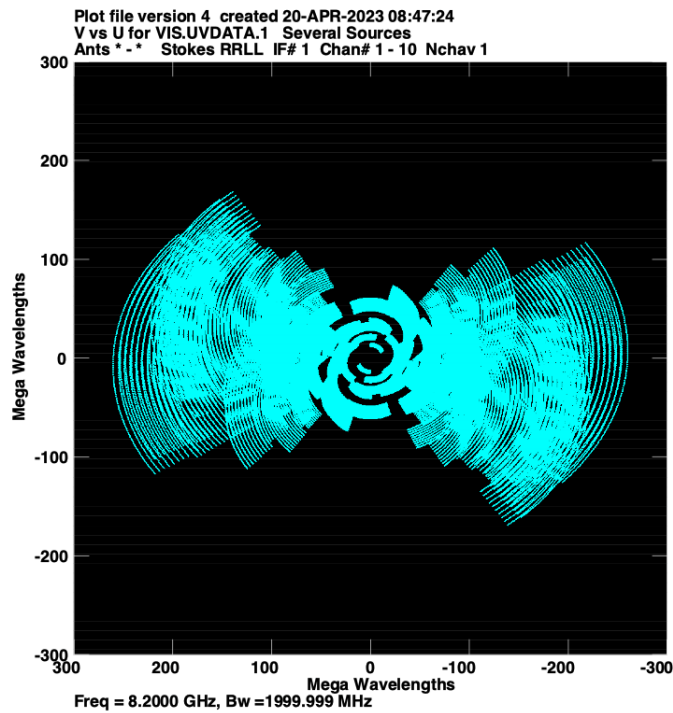
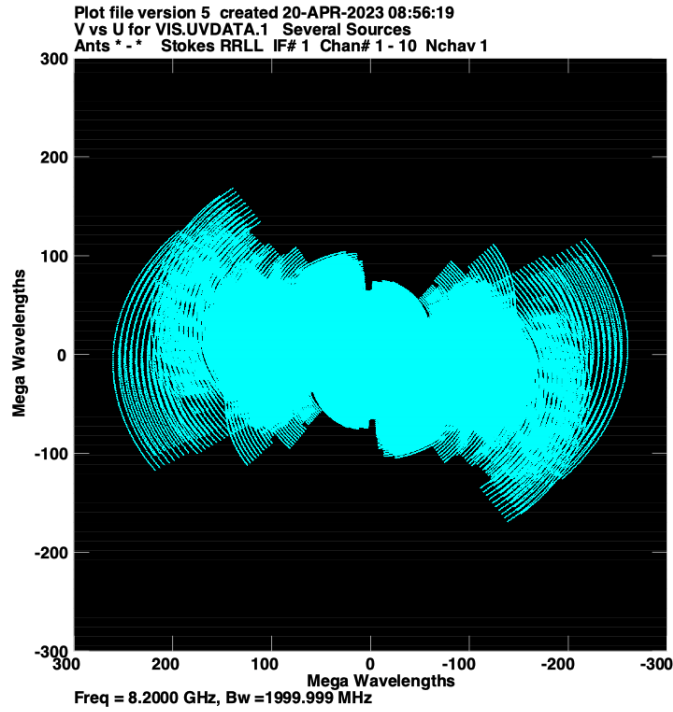


Figure 6: Top: uv-coverage for the simulated observations for LONG++.
 Bottom: uv-coverage for just LONG inter-station baselines.